Conformation and Dynamics of the Pribnow Box Region of the Self-Complementary d(C-G-A-T-T-A-T-A-A-T-C-G) Duplex in Solution

Dinshaw J. Patel*,‡ and Sharon A. Kozlowski

AT&T Bell Laboratories, Murray Hill, New Jersey 07974

Michael Weiss

Chemistry Department, Harvard University, Cambridge, Massachusetts 02138

Ram Bhatt

Molecular Genetics Section, Hoffman-La Roche, Nutley, New Jersey 07110

Received May 15, 1984

ABSTRACT: Nuclear magnetic resonance (NMR) has been used to monitor the conformation and dynamics of the d(C_1-G_2-A_3-T_4-T_5-A_6-T_6-A_5-A_4-T_3-C_2-G_1) self-complementary dodecanucleotide duplex (henceforth called Pribnow 12-mer), which contains a TATAAT Pribnow box and a central core of eight dA·dT base pairs. The exchangeable imino and nonexchangeable base protons have been assigned from one-dimensional intra and inter base pair nuclear Overhauser effect (NOE) measurements. Premelting conformational changes are observed at all the dA·dT base pairs in the central octanucleotide core in the Pribnow 12-mer duplex with the duplex to strand transition occurring at 55 °C in 0.1 M phosphate solution. The magnitude of the NOE measurements between minor groove H-2 protons of adjacent adenosines demonstrates that the base pairs are propeller twisted with the same handedness as observed in the crystalline state. The thymidine imino proton hydrogen exchange at the dA·dT base pairs has been measured from saturation recovery measurements as a function of temperature. The exchange rates and activation barriers show small variations among the four different dA·dT base pairs in the Pribnow 12-mer duplex. The thymidine imino proton exchange rates for the TATAAT Pribnow box in the d(C-G-A-T-T-A-T-A-A-T-C-G) duplex are of similar magnitude to those observed for the TATA box in the d(C-G-C-G-T-A-T-A-C-G-C-G) duplex at 30 °C but are approximately a factor of 3–5 faster than those observed for the AATT segment in the d(C-G-C-G-A-A-T-T-C-G-C-G) duplex at the same temperature. The thymidine imino proton exchange rates in the Pribnow 12-mer are sensitive to basic pH, which suggests that both rate-limiting helix opening and preequilibrium pathways contribute to the hydrogen exchange in the central dA·dT octanucleotide core of the Pribnow 12-mer duplex in solution.

Recent advances in high-resolution NMR instrumentation have resulted in considerable improvement in the resolution of the paired imino proton spectra of transfer RNA (Schimmel & Redfield, 1980; Reid, 1981) and DNA duplexes (Patel et al., 1982a; Kan et al., 1982; Chou et al., 1983; Feigon et al., 1983). Further, the unambiguous assignments of the imino protons to specific positions in the nucleic acid sequence can be made from intra and inter base pair NOE measurements (Roy & Redfield, 1981; Tropp & Redfield, 1981), and this approach has found applications in elucidating structural features in RNA duplexes (Redfield et al., 1981; Hare & Reid, 1982a,b; Heerschap et al., 1982; Broido & Kearns, 1982; Kime & Moore, 1983), DNA duplexes (Patel et al., 1982b,c; 1983a,b; Feigon et al., 1983; Scheek et al., 1983; Reid et al., 1983a; Sanderson et al., 1983; Hare et al., 1983; Weiss et al., 1984), and ligand–DNA complexes (Patel, 1982; Reid et al., 1983b; Alma et al., 1981, 1983; Nick et al., 1982; Kaptein et al., 1982; Pardi et al., 1983; Brown et al., 1984).

These developments set the stage for studies on the hydrogen exchange kinetics of the resolved and assigned imino protons in nucleic acids at the individual base pair level. Redfield and co-workers (1975) have introduced pulsed FT NMR methods for investigating biopolymers in H_2O solution, and the incorporation of time delays readily extends the method to kinetic measurements (Johnston & Redfield, 1977). The saturation recovery method has been applied to investigate hydrogen exchange in transfer RNA (Johnston & Redfield, 1977, 1981; Hurd & Reid, 1980) and DNA duplexes (Pardi & Tinoco, 1982; Pardi et al., 1982), their mismatched and helix interruption analogues (Pardi et al., 1982), and their antibiotic complexes (Pardi et al., 1983). The hydrogen exchange kinetics in DNA restriction fragments had been evaluated earlier from inversion recovery experiments (Early et al., 1981a,b).

We have recently compared the hydrogen exchange parameters for the fully alternating d(C-G-C-G-T-A-T-A-C-G-C-G) duplex (henceforth called TATA 12-mer) and the partially alternating d(C-G-C-G-A-A-T-T-C-G-C-G) duplex (henceforth called AATT 12-mer) and have noted a striking effect of sequence on the opening rate constants of individual dA·dT base pairs in the interior of the dodecanucleotide duplex (Patel et al., 1983c). Specifically the alternating sequence that contains the TATA box exhibits opening rates that are 2.5-fold faster than the related sequence with an AATT segment at the same position (Patel et al., 1983c). Parallel investigations by Lu and co-workers (1983) have also demonstrated faster hydrogen exchange rates for thymidine imino protons in TGTG segments of the *lac* operator fragment.

These investigations are extended below to the self-complementary d(C-G-A-T-T-A-T-A-A-T-C-G) duplex (hence-

‡Present address: Department of Biochemistry and Molecular Biophysics, Columbia University, New York, NY 10032.

0006-2960/85/0424-0936$01.50/0

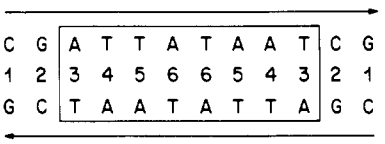

forth called Pribnow 12-mer). This sequence contains the TATAAT segment, a common feature of the Pribnow box region of promoters, which are the sites of initiation of transcription in viral, procaryotic, and eucaryotic DNAs (Pribnow, 1975). Current experimental evidence suggests that RNA polymerase binds to and melts the promoter region, which is rich in dA·dT base pairs (Siebenlist, 1979; Gilbert, 1980).

This paper reports on the application of one-dimensional NOE methods to assign the resolved exchangeable and nonexchangeable base protons in the Pribnow 12-mer duplex. We have evaluated the hydrogen exchange characteristics of the assigned imino protons of the five nonterminal base pairs in the Pribnow 12-mer and compared these rates with parameters in related sequences. The magnitude of the NOEs between the resolved and assigned adenosine H-2 protons on adjacent dA·dT protons in the minor groove of the Pribnow 12-mer duplex has been used to monitor base-pair propeller twisting and elucidate the sign of the propeller twists. The temperature dependence of the nonexchangeable protons provides insights into the premelting and melting transitions of the Pribnow 12-mer duplex in solution. We have published a preliminary report on the application of one-dimensional NOEs to elucidate the sequence dependence of base-pair stacking in d(C-G-A-T-T-A-T-A-A-T-C-G) in solution (Patel et al., 1983b).

Experimental Procedures

NMR Spectroscopy. Proton spectra were recorded on the 498-MHz NMR spectrometer at the Francis Bitter National Magnet Laboratory, MIT, and on a Varian XL-200 spectrometer. Proton spectra in H_2O were accumulated with a Redfield 214 or a time-shared long pulse method (Redfield et al., 1981). The nuclear Overhauser effect and saturation recovery data involving a set of decoupling frequencies or time delays were accumulated in the interleave mode. The experimental conditions are included in the figure captions.

Synthesis. The Pribnow 12-mer was synthesized by the solid-phase phosphotriester method reported previously (Tan et al., 1983). The procedure consists of attaching the 3′-terminal nucleoside of the desired sequence to the polystyrene copolymer support through 1% divinylbenzene linkage. The mononucleotide or dinucleotide coupling units were sequentially added through their 3′-ends to the growing nucleotide chain on the insol. support until the desired sequence was built. The final product was cleaved from the solid support, the protecting groups were deblocked, and the 5′-protected oligomer was passed through a Sephadex G-50 column. The 5′-(dimethoxytrityl)dodecanucleotide was purified by HPLC on μBondapak C_{18} column (Waters) at 84 °C with a linear gradient of 7.5–35% acetonitrile (pH 7.8). The peak eluting at 25% acetonitrile was detritylated with 80% acetic acid, and the oligomer was worked up to remove acetic acid and organic impurities. The deprotected oligomer was further purified under the same HPLC conditions and eluted at 17% acetonitrile (pH 7.8). The organic solvent was evaporated off and the sample dialyzed prior to use. The high-temperature proton NMR spectrum of the Pribnow 12-mer confirmed the purity of the dodecanucleotide.

Concentration. The proton NMR spectra were recorded on 100 A_{260} units of the Pribnow 12-mer in 0.2 mL of 0.1 M phosphate buffer. We could record one-dimensional NOEs readily at this concentration but could not undertake two-dimensional experiments because of signal to noise limitations.

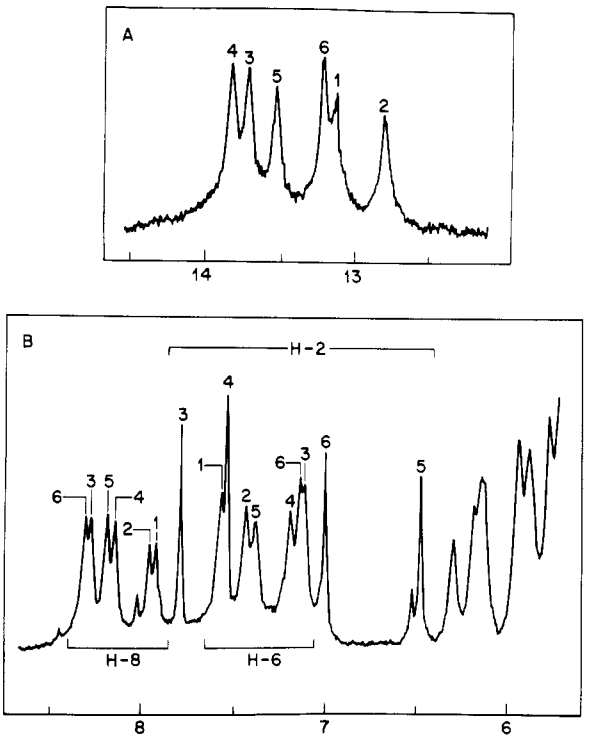

FIGURE 1: The 498-MHz proton NMR spectra of the Pribnow 12-mer in 0.1 M phosphate–2.5 mM EDTA solution. The proton assignments to specific base pairs are designated over the resonances. (A) Imino spectral region (12.5–14.5 ppm) in 5:1 H_2O/D_2O, pH 6.90 at −5 °C. (B) Aromatic spectral region (5.5–8.5 ppm) in D_2O, pH 7.17 at 5 °C.

Table I: Proton Chemical Shifts of Imino Protons in the Pribnow 12-mer Duplex at −5 °C[a]

base pair	chemical shift (ppm)	base pair	chemical shift (ppm)
1	13.13	4	13.83
2	12.82	5	13.53
3	13.72	6	13.22

[a] Buffer was 0.1 M phosphate, 2.5 mM EDTA, and 4:1 H_2O/D_2O, pH 6.90.

Results

There are six unique base pairs in the Pribnow 12-mer sequence, and these are designated dG·dC base pairs 1 and 2 and dA·dT base pairs 3–6 from the ends to the center of the duplex.

Imino Proton Spectra and Assignments. We observe six well-resolved imino protons in the spectrum of the Pribnow 12-mer duplex in 0.1 M phosphate, pH 6.90 at −5 °C (Figure 1A). These imino protons have been assigned from one-dimensional NOE measurements (Patel et al., 1983b), the assignments are listed above the resonances in Figure 1A, and the chemical shifts at −5 °C are listed in Table I.

Temperature Dependence of Shifts. The imino proton spectra in the Pribnow 12-mer duplex in 0.1 M phosphate, pH 6.9, have been investigated as a function of temperature with the spectra between 24 and 44 °C plotted in Figure 2A. The imino proton of dG·dC base pair 2 broadens above 35 °C while the imino protons of dA·dT base pairs 3–6 broaden simultaneously above 45 °C (Figure 2A). The temperature dependence of the imino protons in the Pribnow 12-mer in 0.1 M phosphate is plotted in Figure 2B. The four dA·dT imino

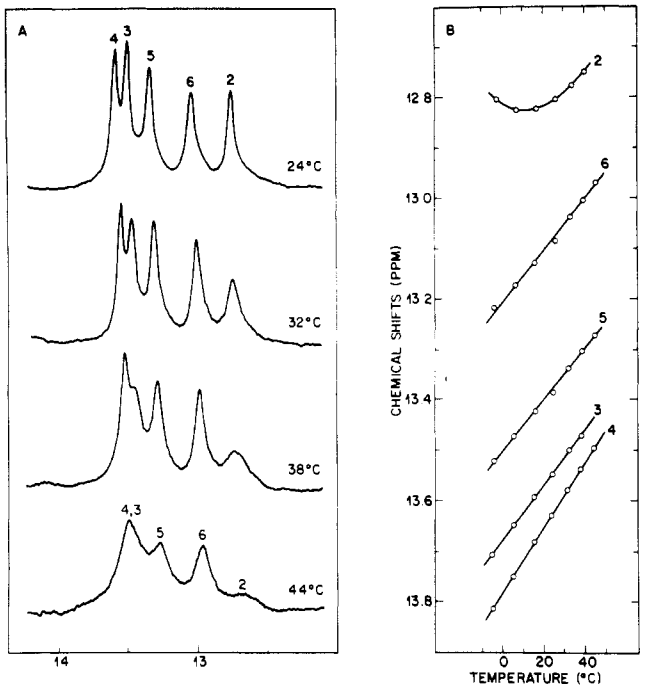

FIGURE 2: (A) The 498-MHz Fourier-transform NMR spectra (12–14 ppm) of the Pribnow 12-mer duplex in 0.1 M phosphate, 2.5 mM EDTA, and 5:1 H_2O/D_2O, pH 6.90 between 24 and 44 °C. The signal to noise of the spectra was improved by applying a 5-Hz line-broadening contribution. The imino proton assignments to specific base pairs are designated over the resonances. (B) Temperature dependence of the imino proton chemical shifts in the Pribnow 12-mer duplex in 0.1 M phosphate solution.

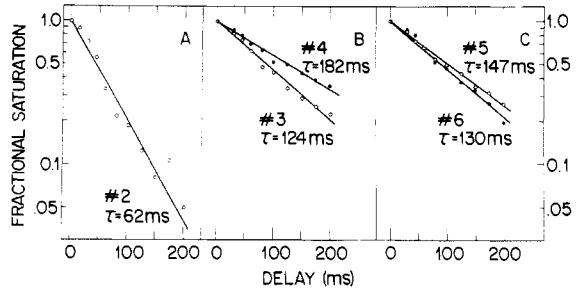

FIGURE 3: Fractional saturation of imino protons of (A) dG·dC base pair 2, (B) dA·dT base pairs 3 and 4, and (C) dA·dT base pairs 5 and 6 in the Pribnow 12-mer duplex in 0.1 M phosphate–5:1 H_2O/D_2O, pH 6.90, as a function of the delay between the saturation and observation pulses in milliseconds at 22.5 °C.

protons all exhibit a similar large temperature dependence in the premelting transition region (Figure 2B).

Saturation Recovery Lifetimes. We have recorded the recovery of magnetization following saturation of the five nonterminal imino protons of the Pribnow 12-mer in 0.1 M phosphate–5:1 H_2O/D_2O, pH 6.90, at various temperatures as a function of the delay between saturation and observation pulses. These experimental data are plotted on semilogarithmic plots of the fractional saturation as a function of the delay for the imino protons of dG·dC base pair 2 (Figure 3A), dA·dT base pairs 3 and 4 (Figure 3B), and dA·dT base pairs 5 and 6 (Figure 3C) in the Pribnow duplex at 22.5 °C. The imino proton of dG·dC base pair 2 toward the end of the duplex recovers its magnetization at the fastest rate while the imino protons of dA·dT base pairs 3–6 recover their magnetization at comparable rates. The slopes of these plots yield saturation recovery lifetimes for the imino protons of the Pribnow 12-mer as shown in Figure 3 and listed in Table II. These lifetimes range between 120 and 180 ms for the imino

Table II: Temperature Dependence of 498-MHz Saturation Recovery Lifetimes of Imino Protons in the Pribnow 12-mer Duplex in 0.1 M Phosphate, pH 6.90

	imino proton lifetimes (ms)				
temp (°C)	2	3	4	5	6
−4.0	154	216	215	224	194
3.0	177	276	273	294	247
10.0	167	260	299	273	251
15.0	142	224	274	230	240
18.7	101	170	239	193	187
22.5	62	124	182	147	130
26.2	38	72	128	80	84
30.0	32	46	77	55	60
33.7		32	51	39	44

Table III: Activation Barriers (18.7–33.7 °C) in the Pribnow 12-mer Duplex[a]

	activation barrier (kcal)			
contribution	3	4	5	6
saturation recovery[b]	22	20	21	18
exchange[c]	30	34	33	29

[a] Buffer is 0.1 M phosphate–5:1 H_2O/D_2O, pH 6.90. [b] The saturation recovery rates between 18.7 and 33.7 °C are directly used to determine the activation energy. [c] The magnetic contribution (saturation recovery rate at 0 °C) is substracted from the saturation recovery rates between 18.7 and 33.7 °C to evaluate the exchange contribution.

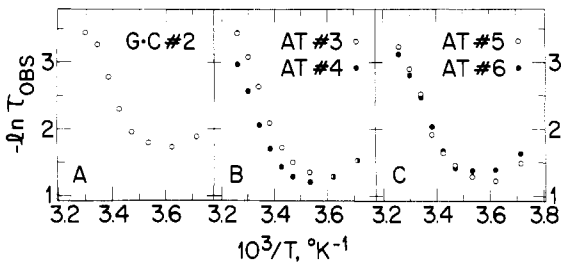

FIGURE 4: Arrhenius plots for inverse of saturation recovery lifetimes at (A) dG·dC base pair 2, (B) dA·dT base pairs 3 and 4, and (C) dA·dT base pairs 5 and 6 in the Pribnow 12-mer duplex in 0.1 M phosphate–5:1 H_2O/D_2O, pH 6.90.

protons of the four dA·dT base pairs at positions 3–6 in the interior of the dodecanucleotide duplex.

Temperature and pH Dependence of Lifetimes. The temperature dependence of the saturation recovery lifetimes for the five nonterminal imino protons in the Pribnow 12-mer in 0.1 M phosphate, pH 6.90, have been measured between −4 and 33.7 °C and are listed in Table II. The experimental data are plotted as the natural logarithm of the inverse of the saturation recovery lifetimes against the inverse of the absolute temperature over this temperature range for the imino protons of dG·dC base pair 2 (Figure 4A), dA·dT base pairs 3 and 4 (Figure 4B), and dA·dT base pairs 5 and 6 (Figure 4C) of the Pribnow 12-mer in 0.1 M phosphate solution.

The saturation recovery rates of the imino protons in the Pribnow 12-mer decrease a bit on increasing the temperature from −4 to 15 °C and then increase dramatically on raising the temperature from 15 to 33.7 °C (Figure 4). The estimated activation energies for saturation recovery from the linear portion of the Arrhenius plots at elevated temperatures are summarized for dA·dT base pairs 3–6 in the Pribnow 12-mer in Table III.

The saturation recovery lifetimes of the imino protons at dA·dT base pairs 3–6 in the Pribnow 12-mer in 0.1 M phosphate have been evaluated at pH 6.9 and 8.5 at 18.7, 22.5, and 26.2 °C and are listed in Table IV. The lifetimes at these internal Pribnow 12-mer base pairs decrease by a factor of

Table IV: pH Dependence of 498-MHz Saturation Recovery Lifetimes of Imino Protons in the Pribnow 12-mer in 0.1 M Phosphate at 18.7, 22.5, and 26.2 °C

	imino proton lifetime (ms)			
	3	4	5	6
18.7 °C				
pH 6.90	170	239	193	187
pH 8.51	73	133	63	85
22.5 °C				
pH 6.90	124	182	147	130
pH 8.51	35	49	31	47
26.2 °C				
pH 6.90	72	128	80	84
pH 8.51		37	30	34

Table V: Nonexchangeable Base Proton Chemical Shifts in the Pribnow 12-mer Duplex in 0.1 M Phosphate–D_2O at 5 °C

		chemical shift (ppm)			
		purine		pyrimidine	
pair	position	H-8	H-2	H-6	H-5
G·C	1	7.93		7.58	5.81
G·C	2	7.95		7.45	5.60
A·T	3	8.28	7.80	7.12	1.26
A·T	4	8.14	7.54	7.18	1.33
A·T	5	8.19	6.50	7.38	1.58
A·T	6	8.31	7.02	7.12	1.34

Table VI: Steady-State NOEs (3-s Saturation)[a] between Adenosine H-2 Protons of the Pribnow 12-mer in 0.1 M Phosphate–D_2O, 5 °C, as a Function of Repetition Delay

repetition delay(s)	pair 3, 4		pair 4, 5		pair 5, 6	
	η_{34}	η_{43}	η_{45}	η_{54}	η_{56}	η_{65}
1	−0.09	−0.09	−0.15	−0.23	−0.38	−0.37
4	−0.13	−0.11	−0.16	−0.26	−0.44	−0.33

[a] The NOE η_{ij} corresponds to saturation of spin i and observation at spin j.

~3 on raising the pH from 6.9 to 8.5 (Table IV).

Adenosine H-2 Protons. The adenosine H-2 proton assignments can be readily determined from the known assignment of the thymidine imino protons in the Pribnow 12-mer on the basis of intra and inter base pair NOE measurements at low temperature (Patel et al., 1983b). The four adenosine H-2's are well resolved in the Pribnow 12-mer, D_2O at 5 °C (Figure 1B), and their chemical shifts are listed in Table V.

We have recently reported on preliminary studies of NOE effects between adenosine H-2 protons in the Pribnow 12-mer in D_2O at low temperature (Patel et al., 1983b). These studies are now complete, and the full details are outlined below. The isolation of the adenosine H-2 protons in the minor groove results in NOEs between adenosine H-2's on adjacent base pairs to the exclusion of other base and sugar protons.

We have monitored the buildup of these adenosine H-2 NOEs at adjacent base pairs for saturation times up to 3 s in the Pribnow 12-mer in D_2O at 5 °C. Steady state is reached at the longer saturation values with some differences in the magnitude of the steady-state values for repetition delays of 1 and 4 s (Table VI). We had used the 1-s repetition delay steady-state NOE values to estimate the interproton distances for the Pribnow 12-mer in our earlier publication (Patel et al., 1983b) but use the longer 4-s repetition delay values in this paper. These steady-state η_{ij} values for the Pribnow 12-mer at 5 °C are summarized in Table VII.

We have measured the selective spin–lattice relaxation rate constants ρ_j at the individual adenosine H-2 protons in the Pribnow 12-mer at 5 °C from selective saturation recovery experiments. These values for individual adenosine H-2 protons at positions 3–6 are listed in Table VII.

Table VII: Cross-Relaxation Rate Constants and Interproton Distances between Adenosine H-2 Protons on Adjacent dA·dT Base Pairs in the Pribnow 12-mer in 0.1 M Phosphate–D_2O at 5 °C

	spin					
pair	i	j	η_{ij}[a]	ρ_j	σ_{ij}	r_{ij}
3, 4	3	4	−0.13	1.29	−0.17	3.8
3, 4	4	3	−0.11	0.97	−0.11	4.1
4, 5	4	5	−0.16	1.63	−0.26	3.55
4, 5	5	4	−0.26	1.29	−0.34	3.4
5, 6	5	6	−0.44	1.31	−0.58	3.1
5, 6	6	5	−0.33	1.63	−0.54	3.15

[a] Repetition delay of 4 s. Resonance i is saturated and the NOE detected at resonance j.

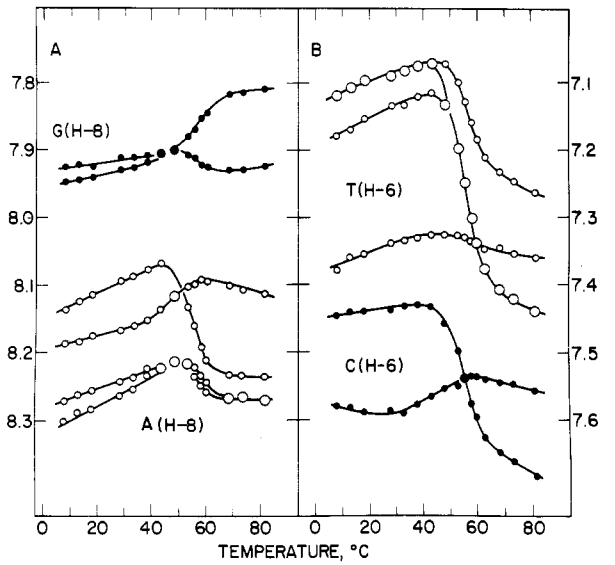

FIGURE 5: Temperature dependence of 200-MHz proton chemical shifts of (A) the guanosine H-8 and adenosine H-8 protons and (B) the thymidine H-6 and cytidine H-6 protons in the Pribnow 12-mer in 0.1 M phosphate, 2.5 mM EDTA, and D_2O between 5 and 85 °C.

The cross-relaxation rate constant $\sigma_{ij} = \eta_{ij}\rho_j$ can then be measured from the product of the steady-state NOE (η_{ij}) and the selective spin–lattice relaxation rate constant (ρ_j) for the Pribnow 12-mer at 5 °C (Table VII). It is readily apparent that the σ_{ij} values decrease in the order $\sigma_{56} \sim \sigma_{65} > \sigma_{45} \sim \sigma_{54} > \sigma_{34} \sim \sigma_{43}$ for the dodecanucleotide at low temperature (Table VII).

The interproton distance r_{ij} can be measured from a knowledge of σ_{ij} and τ_c, the correlation time for isotropic tumbling by (Redfield et al., 1981)

$$\sigma_{ij} = -\frac{5.68 \times 10^{10}}{r_{ij}^6}\tau_c$$

for the condition $\omega\tau_c \gg 1$, which is met in this case for studies at 498 MHz ($\omega = 3.1 \times 10^9$ rad/s). We use a value of τ_c = 9 ns for the Pribnow 12-mer at 5 °C on the basis of an earlier report of τ_c = 7 ns measured for a dodecanucleotide at 21 °C (Early et al., 1981a). The interproton distances σ_{ij} between adjacent adenosine H-2's are strikingly different in the Pribnow 12-mer at 5 °C with the shortest distance observed between base pairs 5 and 6 and the longest between base pairs 3 and 4 (Table VII).

Purine Nonexchangeable Protons. The two guanosine H-8 (7.9–8.0 ppm), the four adenosine H-8 (8.1–8.3 ppm), and adenosine H-2 protons are well resolved in the Pribnow 12-mer in the duplex state (Figure 1B) and can be monitored as a function of temperature through the premelting and melting

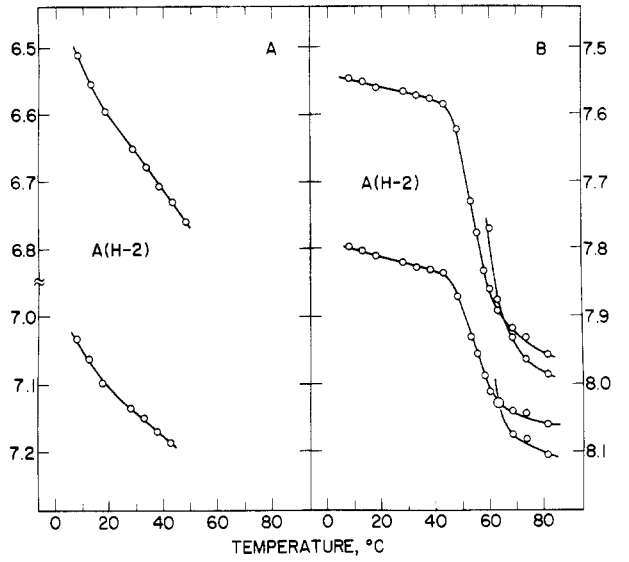

FIGURE 6: Temperature dependence of 200-MHz proton chemical shifts of the adenosine H-2 protons in the Pribnow 12-mer in 0.1 M phosphate, 2.5 mM EDTA, and D_2O between 5 and 85 °C.

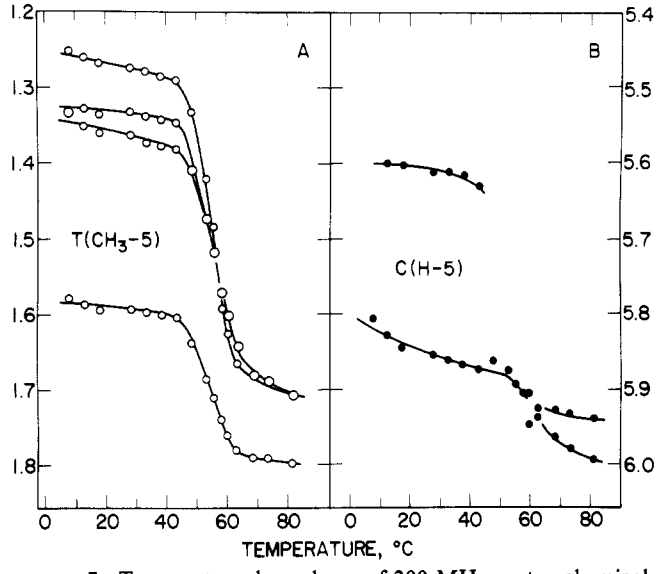

FIGURE 7: Temperature dependence of 200-MHz proton chemical shifts of (A) the thymidine CH_3-5 and (B) the cytidine H-5 protons in the Pribnow 12-mer in 0.1 M phosphate, 2.5 mM EDTA, and D_2O between 5 and 85 °C.

transitions. The majority of these purine resonances shift as average peaks (at 200 MHz) through the melting transitions with a midpoint of ~55 °C for the Pribnow 12-mer in 0.1 M phosphate solution (Figures 5–7). The adenosine H-2 protons at ~6.5 (position 5) and ~7.0 ppm (position 6) in the Pribnow 12-mer at 5 °C exhibit large downfield premelting transition shifts on raising the temperature (Figure 6A) and are in slow exchange with their strand values (~8.1 ppm) through the melting transition.

Pyrimidine Nonexchangeable Protons. The two cytidine H-6 protons (7.4–7.6 ppm), the four thymidine H-6 protons (7.1–7.4 ppm), the two cytidine H-5 protons (5.6–5.8 ppm), and the four thymidine CH_3-5 protons (1.2–1.6 ppm) are resolved from each other in the Pribnow 12-mer in the duplex state (Figure 1B). These resonances shift as average peaks (at 200 MHz) with temperature and exhibit a transition midpoint of 55 °C for the dodecanucleotide duplex in 0.1 M phosphate solution (Figures 5B and 7A). The base proton chemical shifts in the Pribnow 12-mer in the duplex state at

Table VIII: Transition Midpoints Measured at the Nonexchangeable Base Protons in the Pribnow 12-mer in 0.1 M Phosphate–D_2O

		transition midpoint (°C)			
		purine		pyrimidine	
pair	position	H-8	H-2	H-6	H-5
G·C	1				
G·C	2			56.5	
A·T	3		55.0	55.0	56.0
A·T	4	55.0	55.5	55.5	56.0
A·T	5			54.0	
A·T	6			56.5	56.0

Table IX: One-Dimensional Intra and Inter Base Pair NOEs at Nonexchangeable Base Protons on Saturation of Thymidine CH_3-5 Protons in the Pribnow 12-mer Duplex in 0.1 M Phosphate at 5 °C[a]

saturate	NOEs observed at			
T CH_3-5	A H-8	C H-6	T CH_3-5	T H-6
1.26 (3)	8.14 (4)	7.45 (2)		7.11 (3)
1.33 (4)	8.28 (3)		1.58 (5)	7.18 (4)
				7.38 (5)
1.34 (6)	8.31 (6)			7.13 (6)
1.58 (5)			1.33 (4)	7.38 (5)
				7.18 (4)

[a] The assignments are designated in parentheses.

5 °C and their melting transitions midpoints are summarized in Tables V and VIII, respectively.

Nonexchangeable Proton Assignments. The nonexchangeable base protons can be assigned by monitoring the NOEs amongst pyrimidine H-5/CH_3-5 and purine H-8 protons on adjacent bases on the same strand in the Pribnow duplex. Examination of molecular models of right-handed B DNA indicates that the interproton distances are <4 Å between H-5/CH_3-5 protons on adjacent pyrimidines in the pyrimidine(3′–5′)pyrimidine sequence, between H-8 protons on adjacent purines in the purine(3′–5′)purine sequence, and between the purine H-8 and pyrimidine H-5/CH_3-5 on adjacent bases in the purine(3′–5′)pyrimidine sequence (Patel et al., 1983a; Feigon et al., 1983; Reid et al., 1983a; Hare et al., 1983; Weiss et al., 1984).

Thus, one predicts that the saturation of the thymidine CH_3-5 at position 4 should result in NOEs at the adenosine H-8 at position 3 and the thymidine CH_3-5 at position 5 in the same strand in the Pribnow sequence. Also, one predicts that saturation of the thymidine CH_3-5 at position 3 should result in NOEs at the adenosine H-8 at position 4 and the cytidine H-6 at position 2 on the same strand in the Pribnow 12-mer sequence.

By contrast, the interproton distance is >4 Å between the pyrimidine H-5/CH_3-5 and purine H-8 on adjacent bases in the pyrimidine(3′–5′)purine sequence from molecular models of right-handed B DNA. Thus, saturation of the thymidine CH_3-5 at position 5 will not result in an observable NOE at the adenosine H-8 of base pair 6 in the Pribnow 12-mer sequence. Three of the four thymidines and adenosines in the Pribnow 12-mer sequence are in dA(3′–5′)dT steps resulting in NOEs between the purine H-8 and thymidine CH_3-5's on adjacent bases on the same strand and can be differentiated from the remaining thymidine CH_3-5 at 1.58 ppm (assigned to position 5) and the adenosine H-8 at 8.19 ppm (assigned to position 5), which do not show the NOE effects (Table IX and X).

The thymidine CH_3-5 at 1.26 ppm is assigned to position 3 since it shows an NOE to the 7.45 ppm cytidine H-6 proton (assigned to position 2) and the 8.14 ppm adenosine H-8 proton (assigned to position 4) (Figure 8B and Table IX). The

Table X: One-Dimensional Intra and Inter Base Pair NOEs at Nonexchangeable Base Protons on Saturation of Adenosine H-8 Protons in the Pribnow 12-mer Duplex in 0.1 M Phosphate at 5 °C[a]

	NOEs observed at	
saturate A H-8	T CH_3-5	G H-8
8.14 (4)	1.26 (3)	
8.19 (5)		
8.28 (3)	1.33 (4)	7.95 (2)
8.31 (6)	1.34 (6)	

[a] The assignments are designated in parentheses.

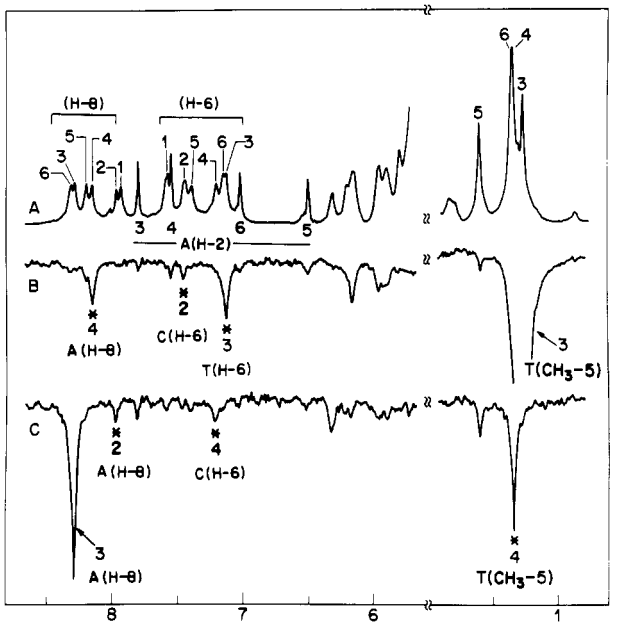

FIGURE 8: (A) The 498-MHz proton NMR spectrum (5.5–8.5 ppm; 1–2 ppm) of the Pribnow 12-mer in 0.1 M phosphate, 2.5 mM EDTA, and D_2O, pH 7.17 at 5 °C. Difference spectra following 1-saturation of (A) the 1.26 ppm thymidine CH_3-5 of base pair 3 and (B) the 8.28 ppm adenosine H-8 of base pair 3. The saturated resonance is designated by an arrow, and the observed NOEs are designated by asterisks.

thymidine CH_3-5 at 1.33 ppm is assigned to position 4 since it shows an NOE to the 1.58 ppm thymidine CH_3-5 proton (assigned to position 5) and the 8.28 ppm adenosine H-8 proton (assigned to position 3) (Table IX.) The remaining thymidine CH_3-5 at 1.34 ppm is assigned to position 6 and shows an NOE at the 8.31 ppm adenosine H-8, which is also assigned to base pair 6 (Table IX).

These conclusions are verified by saturating the adenosine H-8 protons and monitoring the NOEs at the thymidine CH_3-5 protons (Table X). Thus, the adenosine H-8 proton at 8.28 ppm is assigned to position 3 since it shows an NOE to the 7.95 ppm guanosine H-8 proton (assigned to position 2) and the 1.33 ppm thymidine CH_3-5 proton (assigned to position 4) in the Pribnow 12-mer sequence (Figure 8C and Table X).

We also observe NOEs between the H-6 and CH_3-5 on the same thymidine and the H-6 and H-5 on the same cytidine in the dodecanucleotide duplex. This completes the assignment of all the base protons in the Pribnow 12-mer, and these are listed for the duplex state at 5 °C in Figure 8A and Table V.

The only possible ambiguity in the assignments arises due to the poor resolution of the thymidine CH_3-5 resonances at 1.33 and 1.34 ppm in the Pribnow 12-mer spectrum at 5 °C. The inherent difficulties with selective one-dimensional saturation of two partially resolved peaks can be overcome from two-dimensional NOE experiments. We have been unable to get good NOESY spectra on the limited amounts of Pribnow 12-mer at our disposal at this time.

Discussion

Assignments. We observe well-resolved resonances for the imino (Figure 1A) and nonexchangeable (Figure 1B) proton spectra of the Pribnow 12-mer duplex in aqueous solution. These resolved resonances have been assigned from one-dimensional NOEs between protons on the same base pair and between protons on adjacent base pairs. The chemical shifts of the assigned imino and nonexchangeable base protons are listed in Tables I and V, respectively.

Premelting Transition. We have monitored the assigned protons in the Pribnow 12-mer in 0.1 M phosphate between 0 and 80 °C. Large premelting chemical shift changes are observed at the four thymidine imino protons (Figure 2B) and two adenosine H-2 protons (Figure 6A) in the Pribnow 12-mer for which the chemical shift difference between duplex and strand states is >1 ppm. Smaller premelting shifts are observed at the four adenosine H-8 (Figure 5A), four thymidine H-6 (Figure 5B), two adenosine H-2 (Figure 6B), and four thymidine CH_3-5 (Figure 7A) resonances in the Pribnow 12-mer for which the chemical shift differences between duplex and strand states is <0.5 ppm. By contrast, the proton chemical shifts of the base protons of the nonterminal dG·dC base pair in the Pribnow 12-mer exhibit very small chemical shift changes between 0 and 40 °C (Figures 5A,B and 7B).

These results suggest changes in the base-pair overlaps in the dA·dT-rich octanucleotide core of the Pribnow 12-mer with temperature in the premelting transition region. This could reflect changes in the extent of base-pair propeller twisting of dA·dT base pairs and/or changes in groove dimensions resulting from disruption of ordered water in the minor groove with increasing temperature (Dickerson et al., 1983).

Melting Transition. The majority of the nonexchangeable base proton resonances in the Pribnow 12-mer can be followed as average peaks through the duplex to strand transitions. The transition midpoint can be measured for several of these markers, and we estimate t_m values of 55 ± 1 °C at base pairs 2–6 in the Pribnow 12-mer in 0.1 M phosphate solution (Table VIII). We are unable to measure the t_m values for base pair 1 due to the small chemical shift difference between duplex and strand states. The results suggest that the 10 nonterminal base pairs in the Pribnow 12-mer melt in a cooperative manner during the helix to coil transition.

The observed transition midpoint of 55 °C for the d(C-G-A-T-T-A-T-A-A-T-C-G) duplex in 0.1 M phosphate may be compared with midpoints of 72 °C for the d(C-G-C-G-A-A-T-T-C-G-C-G) and d(C-G-C-G-T-A-T-A-C-G-C-G) duplexes in 0.1 M phosphate reported previously (Patel et al., 1983c). This demonstrates that the replacement of four dG-dC base pairs by four dA-dT base pairs results in a 17 °C destabilization of the duplex to strand transition.

Propeller Twists. The adenosine H-2 selective spin–lattice relaxation rates and inter base pair NOE parameters can be interpreted to yield interproton distances between adenosine H-2 protons on adjacent base pairs (Table VII). The experimentally measured distances are ~4.0 Å for the (dA_3-dT_4)·(dA_4-dT_3) step, ~3.5 Å for the (dT_4-dT_5)·(dA_5-dA_4) step, and ~3.1 Å for the (dT_5-dA_6)·(dT_6-dA_5) step in the Pribnow 12-mer at 5 °C (Table VII).

The progression of distances reflects the consequences of base-pair propeller twisting (Levitt, 1978; Hogan et al., 1978) of defined handedness (Dickerson & Drew, 1981; Calladine, 1982) as shown in Chart I, where the separation between H-2 protons on adjacent adenosines decreases in the order (dA_3-dT_4)·(dA_4-dT_3) > (dT_4-dT_5)·(dA_5-dA_4) > (dT_5-dA_6)·

Chart I

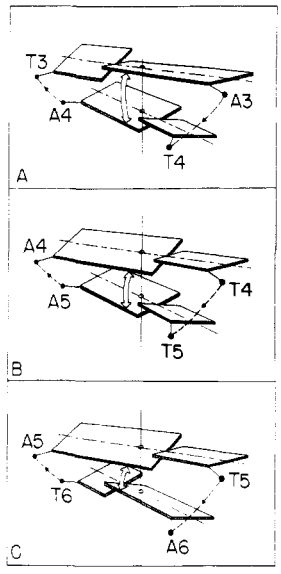

(dT_6-dA_5). These distances are available for the Arnott–Chandrasekaran model of right-handed DNA with a 13° propeller twist of the same handedness as in Chart I (Arnott et al., 1983) and decreases for the same dinucleotide steps in the order 4.36 Å > 3.63 Å > 2.94 Å. It should be noted that the order of distances between adjacent adenosine H-2 protons would be reversed if the handedness of the propeller twist had an opposite sign from that shown in Chart I.

Hydrogen Exchange Rates. It has been shown from hydrogen–deuterium exchange stop-flow measurements that the exchange kinetics of the Watson–Crick imino protons are sensitive markers of the dynamics of the base-pair opening in the interior of nucleic acid duplexes (Mandel et al., 1979). We have used the saturation recovery NMR method (Johnston & Redfield, 1977) to measure the hydrogen exchange behavior of individual base pairs in the Pribnow 12-mer duplex in 0.1 M phosphate as a function of temperature at pH 6.9 (Table II) and as a function of pH at several temperatures (Table IV). The measured saturation recovery rate is the sum of the magnetic spin–lattice relaxation rate and the chemical exchange rate with unperturbed solvent water. The saturation recovery rates of the Pribnow 12-mer in 0.1 M phosphate, pH 6.9, decrease gradually from −4 to 15 °C (Table II, Figure 4) and are predominantly a measure of the magnetic spin–lattice relaxation rate in this low-temperature region. The small temperature dependence of the recovery rates reflects the effect of viscosity changes on the rotational correlation times. By contrast, the saturation recovery rates increase dramatically between 15 and 34 °C (Table II, Figure 4) and are predominately a measure of the chemical exchange rate in this elevated temperature region. We note that the thymidine imino protons at positions 3–6 exhibit small variations in the hydrogen exchange lifetimes at a given temperature between 15 and 34 °C (Table II and Figure 4) and small variations in the activation barriers in this temperature range (Table III and Figure 4).

Promoter Regions. We have previously established a sequence dependence of the hydrogen exchange characteristics of dA·dT base pairs in oligonucleotide duplexes (Patel et al., 1983b). Thus, the thymidine imino protons in the d(C_1-G_2-C_3-G_4-T_5-A_6-T_6-A_5-C_4-G_3-C_2-G_1) TATA 12-mer duplex exhibit hydrogen exchange rates that are a factor if 2–3 faster than the corresponding protons in the d(C_1-G_2-C_3-G_4-A_5-A_6-T_6-T_5-C_4-G_3-C_2-G_1) AATT 12-mer duplex (Patel et al., 1983b). These exchange lifetimes are summarized for dA·dT base pairs 5 and 6 in the TATA 12-mer (pH 6.54) and in the AATT 12-mer (pH 6.95) in 0.1 M phosphate at 30 °C in Table XI. This table also includes the exchange lifetimes for dA·dT base pairs 3–6 in the Pribnow 12-mer (pH 6.9) in 0.1 M phosphate at 30 °C.

Table XI: 498-MHz Saturation Recovery Lifetimes of Thymidine Imino Protons of dA·dT Base Pairs in Dodecanucleotide Duplexes in 0.1 M Phosphate Solution at 30 °C

	imino proton lifetime (ms)			
	3	4	5	6
AATT 12-mer[a]			184	310
TATA 12-mer[b]			60	94
Pribnow 12-mer[c]	46	77	55	60

[a] 4:1 H_2O/D_2O, pH 6.95. [b] 4:1 H_2O/D_2O, pH 6.54. [c] 5:1 H_2O/D_2O, pH 6.90.

Scheme I

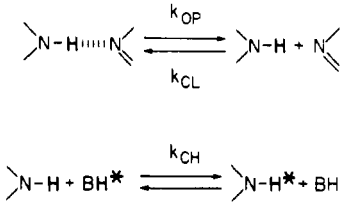

We note that all four thymidine imino protons at positions 3–6 in the Pribnow 12-mer exhibit exchange lifetimes similar to values at positions 5 and 6 in the TATA 12-mer but are much shorter than the corresponding values in the AATT 12-mer (Table XI). Thus, faster hydrogen exchange rates are observed for the TATA box and the TATAAT Pribnow box in comparison to the related AATT sequence in dodecanucleotide duplexes. It should be noted that Lu and collaborators have observed faster exchange rates for thymidine imino protons in GTG segments in regulatory sequences (Lu et al., 1983).

Hydrogen Exchange Pathways. The hydrogen exchange parameters for dA·dT base pairs 5 and 6 in the AATT 12-mer and TATA 12-mer are essentially independent of pH between 6.5 and 8.5 (Pardi et al., 1982; Patel et al., 1983c). This demonstrates that the exchange rate is a direct measure of the transient duplex opening rate (Scheme I), $k_{EX} = k_{OP}$ (Teitelbaum & Englander, 1975a,b; Mandal et al., 1979).

By contrast, we observe a pH dependence for the exchange rates of dA·dT base pairs 3–6 in the Pribnow 12-mer with the exchange rates increasing by a factor of ~3 on raising the pH from 6.9 to 8.5 (Table IV). If exchange occurs through a preequilibrium pathway (Scheme I)

$$k_{EX} = \frac{k_{OP}}{k_{CL}} k_{CH}[BH]$$

the exchange rate is directly related to the base concentration (Teitelbaum & Englander, 1975a,b; Mandal et al., 1982).

The observed increase in exchange rates by a factor of 3 on raising the pH by 1.6 units indicates that both helix opening and prequilibrium pathways contribute to the exchange of the block of eight dA·dT base pairs in the Pribnow 12-mer duplex. These results demonstrate that base pairs in dA·dT-rich regions in the interior of duplexes can exchange, in part, through a preequilibrium pathway similar to the earlier observation for base pairs at the ends of duplexes (Patel & Hilbers, 1975; Pardi et al., 1982).

SUMMARY

The d(C-G-A-T-T-A-T-A-A-T-C-G) Pribnow 12-mer contains an internal core of eight dA·dT base pairs. High-

resolution proton NMR measurements permit us to monitor the structure and hydrogen exchange kinetics at the individual base-pair level and search for sequence-dependent effects in the conformation and dynamics of nucleic acids. Our one-dimensional NOE experiments support base-pair propeller twisting of defined handedness in solution and demonstrate fast hydrogen exchange kinetics for the TATAAT Pribnow sequence in the dodecanucleotide duplex. We observe a noncooperative premelting conformational transition in the dA·dT-rich octanucleotide core of the duplex and can monitor a cooperative helix–coil transition at the 10 nonterminal base pairs.

ACKNOWLEDGMENTS

We acknowledge helpful discussion with Dr. Horace Drew on base-pair propeller twisting. Dr. R. Chandrasekaran computed the interproton distances between adenosine H-2 protons on adjacent base pairs in the Pribnow 12-mer on the basis of the Arnott–Chandrasekaran model of B DNA (Arnott et al., 1983). Prof. R. E. Dickerson kindly gave permission to use his drawings of propeller-twisted base pairs (Dickerson, 1983), which are the basis for Chart I. The high-field NMR experiments were performed at the NMR facility for Biomedical Research at the Francis Bitter National Magnet Laboratory, Massachusetts Institute of Technology. The NMR facility is supported by Grant RR0095 from the Division of Research Resources of the National Institutes of Health and by the National Science Foundation under Contract C-670.

Registry No. Pribnow 12-mer, 86343-17-1.

REFERENCES

Alma, N. C. M., Harmsen, B. J. M., Hull, W. E., van der Marel, G., van Boom, J. H., & Hilbers, C. W. (1981) *Biochemistry 20*, 4419–4428.

Alma, N. C. M., Harmsen, B. J. M., van Boom, J. H., van der Marcel, G., & Hilbers, C. W. (1983) *Biochemistry 22*, 2104–2115.

Arnott, S., Chandrasekaran, R., Hall, I. H. Puigjaner, L. C., Walker, J. K., & Wang, M. (1983) *Cold Spring Harbor Symp. Quant. Biol. 47*, 53–65.

Broido, M. S., & Kearns, D. R. (1982) *J. Am. Chem. Soc. 104*, 5207–5216.

Brown, S. C., Mullis, K., Levenson, C., & Shafer, R. H. (1984) *Biochemistry 23*, 403–408.

Calladine, C. R. (1982) *J. Mol. Biol. 161*, 343–362.

Chou, S. H., Hare, D. R., Wemmer, D. E., & Reid, B. R. (1983) *Biochemistry 22*, 3037–3041.

Dickerson, R. E. (1983) *J. Mol. Biol. 166*, 419–441.

Dickerson, R. E., & Drew, H. R. (1981) *J. Mol. Biol. 149*, 761–786.

Dickerson, R. E., Drew, H. R., Conner, B. N., Kopka, M. L., & Pjura, P. E. (1983) *Cold Spring Harbor Symp. Quant. Biol. 47*, 13–24.

Early, T. A., Kearns, D. R., Hillen, W., & Wells, R. D. (1981a) *Biochemistry 20*, 3756–3764.

Early, T. A., Kearns, D. R., Hillen, W., & Wells, R. D. (1981b) *Biochemistry 20*, 3764–3769.

Feigon, J., Wright, J. M., Denny, W., Leupin, W., & Kearns, D. R. (1983) *Cold Spring Harbor Symp. Quant. Biol. 47*, 207–217.

Fritzche, H., Kan, L. S., & T'so, P. O. P. (1983) *Biochemistry 22*, 277–280.

Gilbert, W. (1980) *Cell (Cambridge, Mass.) 20*, 269–281.

Hare, D. R., & Reid, B. R. (1982a) *Biochemistry 21*, 1835–1842.

Hare, D. R., & Reid, B. R. (1982b) *Biochemistry 21*, 5129–5135.

Hare, D. R., Wemmer, D. E., Chou, S. H., Drobny, G., & Reid, B. R. (1983) *J. Mol. Biol. 171*, 319–336.

Heerschap, A., Haasnoot, C. A. G., & Hilbers, C. W. (1982) *Nucleic Acids Res. 10*, 6981–7000.

Hogan, M., Dattagupta, N., & Crothers, D. M. (1978) *Proc. Natl. Acad. Sci. U.S.A. 75*, 195–199.

Hurd, R. E., & Reid, B. R. (1980) *J. Mol. Biol. 142*, 181–193.

Johnston, P. D., & Redfield, A. G. (1977) *Nucleic Acids Res. 4*, 3599–3615.

Johnston, P. D., & Redfield, A. G. (1981) *Biochemistry 20*, 3996–4006.

Kan, L. S., Cheng, D. M., Jayaraman, K., Lentzinger, E. E., Miller, P. S., & T'so, P. O. P. (1982) *Biochemistry 21*, 6723–6732.

Kaptein, R., Scheek, R. M., Zuiderweg, E. R. P., Boelens, R., Klappe, K. J. M., van Boom, J. H., Rüterjans, H., & Beyreuther, K. (1983) *Structure and Dynamics: Nucleic Acids and Proteins* (Clementi, E., & Sarma, R. H., Eds.) pp 209–225, Academic Press, New York.

Kime, M. J., & Moore, P. B. (1983) *Biochemistry 22*, 2615–2622.

Levitt, M. (1978) *Proc. Natl. Acad. Sci. U.S.A. 75*, 640–644.

Lu, P., Cheung, S., & Arndt, K. (1983) *J. Biomol. Struct. Dyn. 1*, 509–521.

Mandal, C., Kallenbach, N. R., & Englander, S. W. (1979) *J. Mol. Biol. 135*, 391–411.

Nick, H., Arndt, K., Boschelli, F., Jarema, M. A. C., Lillis, M., Sadler, J., Caruthers, M., & Lu, P. (1982) *Proc. Natl. Acad. Sci. U.S.A. 79*, 218–222.

Pardi, A., & Tinoco, I., Jr. (1982) *Biochemistry 21*, 4686–4693.

Pardi, A., Morden, K., Patel, D. J., & Tinoco, I., Jr. (1982) *Biochemistry 21*, 6567–6574.

Pardi, A., Morden, K. M., Patel, D. J., & Tinoco, I., Jr. (1983) *Biochemistry 22*, 1107–1113.

Patel, D. J. (1982) *Proc. Natl. Acad. Sci. U.S.A. 79*, 6424–6428.

Patel, D. J., & Hilbers, C. W. (1975) *Biochemistry 14*, 2651–2656.

Patel, D. J., Pardi, A., & Itakura, K. (1982a) *Science (Washington, D.C.) 216*, 581–590.

Patel, D. J., Kozlowski, S. A., Marky, L. A., Broka, C., Rice, J. A., Itakura, K., & Breslauer, K. J. (1982b) *Biochemistry 21*, 428–436.

Patel, D. J., Kozlowski, S. A., Nordheim, A., & Rich, A. (1982c) *Proc. Natl. Acad. Sci. U.S.A. 79*, 1413–1417.

Patel, D. J., Kozlowski, S. A., Ikuta, S., Itakura, K., Bhatt, R., & Hare, D. R. (1983a) *Cold Spring Harbor Symp. Quant. Biol. 47*, 197–206.

Patel, D. J., Kozlowski, S. A., & Bhatt, R. (1983b) *Proc. Natl. Acad. Sci. U.S.A. 80*, 3908–3912.

Patel, D. J., Ikuta, S., Kozlowski, S., & Itakura, K. (1983c) *Proc. Natl. Acad. Sci. U.S.A. 80*, 2184–2188.

Pribnow, D. (1975) *J. Mol. Biol. 99*, 419–443.

Redfield, A. G., Kunz, S. D., & Ralph, E. K. (1975) *J. Magn. Reson. 19*, 114–117.

Redfield, A. G., Roy, S., Sanchez, V., Tropp, J., & Figueroa, N. (1981) in *Second SUNYA Conference on Biomolecular Sterodynamics* (Sarma, R. H., Ed.) pp 195–208, Adenine Press, New York.

Reid, B. R. (1981) *Annu. Rev. Biochem. 50*, 969–996.

Reid, D. G., Salisbury, S. A., Bellard, S., Shakked, Z., & Williams, D. H. (1983a) *Biochemistry 22*, 2019–2025.

Reid, D. G., Salisbury, S. A., & Williams, D. H. (1983b) *Biochemistry 22*, 1377-1385.
Roy, S., & Redfield, A. G. (1981) *Nucleic Acids Res. 9*, 7073-7078.
Sanderson, M. R., Mellema, J. R., van der Marel, G. A., Wille, G., van Boom, J. H., & Altona, C. (1983) *Nucleic Acids Res. 11*, 3333-3346.
Scheek, R. M., Zuiderweg, E. R. P., Klappe, K. J. M., van Boom, J. H., Kaptein, R., Ruterjans, H., & Beyreuther, K. (1983) *Biochemistry 22*, 228-235.
Schimmel, P. R., & Redfield, A. G. (1980) *Annu. Rev. Biophys. Bioeng. 9*, 181-221.
Siebenlist, U. (1979) *Nature (London) 279*, 651-652.
Tan, Z. K., Ikuta, S., Huang, T., Dugaiczyk, A., & Itakura, K. (1983) *Cold Spring Harbor Symp. Quant. Biol. 47*, 383-391.
Teitelbaum, H., & Englander, S. W. (1975a) *J. Mol. Biol. 92*, 57-78.
Teitelbaum, H., & Englander S. W. (1975b) *J. Mol. Biol. 92*, 79-92.
Tropp, J., & Redfield, A. G. (1981) *Biochemistry 20*, 2133-2140.
Weiss, M., Patel, D. J., Sauer, R. T., & Karplus, M. (1984) *Proc. Natl. Acad. Sci. U.S.A. 81*, 130-134.

Use of Intermediate Partitioning To Calculate Intrinsic Isotope Effects for the Reaction Catalyzed by Malic Enzyme†

Charles B. Grissom and W. W. Cleland*

Department of Biochemistry, University of Wisconsin, Madison, Wisconsin 53706
Received August 21, 1984

ABSTRACT: For those enzymes that proceed via a stepwise reaction mechanism with a discrete chemical intermediate and where deuterium and ^{13}C isotope effects are on separate steps, a new method has been developed to solve for the intrinsic deuterium and ^{13}C kinetic isotope effects that relies on directly observing the partitioning of the intermediate between the forward and reverse directions. This observed partitioning ratio, along with the values of the primary deuterium, tritium, and ^{13}C kinetic isotope effects on V/K for the substrate with the label being followed, allows an exact solution for the intrinsic deuterium and ^{13}C isotope effects, the forward commitment for the deuterium-sensitive step, and the partition ratio for the intermediate in the reaction. This method allows portions of the reaction coordinate diagram to be defined precisely and the relative energy levels of certain activation barriers to be assigned exactly. With chicken liver triphosphopyridine nucleotide (TPN) malic enzyme activated by Mg^{2+}, the partitioning of oxalacetate to pyruvate vs. malate in the presence of TPNH, 0.47, plus previously determined isotope effects gives an intrinsic deuterium isotope effect of 5.7 on hydride transfer and a ^{13}C isotope effect of 1.044 on decarboxylation. Reverse hydride transfer is 10 times faster than decarboxylation, and the forward commitment for hydride transfer is 3.3. The ^{13}C isotope effect is not significantly different with reduced acetylpyridine adenine dinucleotide phosphate replacing TPNH (although the pyruvate/malate partitioning ratio for oxalactate is now 9.9), but replacement of Mg^{2+} by Mn^{2+} raises the value to 1.065 (partition ratio 0.99).

TPN malic enzyme catlayzes the oxidative decarboxylation of L-malate with concomitant reduction of triphosphopyridine nucleotide (TPN):[1]

$$\text{L-malate} + \text{TPN}^+ \overset{M^{2+}}{\rightleftharpoons} \text{pyruvate} + CO_2 + \text{TPNH} \quad (1)$$

The enzyme will use several divalent metal cations, most commonly Mg^{2+} and Mn^{2+}. The enzyme will also utilize the alternate nucleotide 3-acetylpyridine adenine dinucleotide phosphate. The kinetic mechanism of pigeon liver TPN malic enzyme was shown by Hsu et al. (1967) to be ordered sequential with TPN adding before malate, followed by release of CO_2, pyruvate, and then TPNH.

In addition to the oxidative decarboxylation of malate, the enzyme will also catalyze the TPNH-dependent reduction of oxalacetate to malate and the decarboxylation of oxalacetate to pyruvate and CO_2 (Viega Salles & Ochoa, 1950). Because of this, it has long been believed that dehydrogenation of malate in the central complex occurs first to yield an oxalacetate intermediate of finite lifetime, which is then decarboxylated to yield CO_2 and pyruvate:

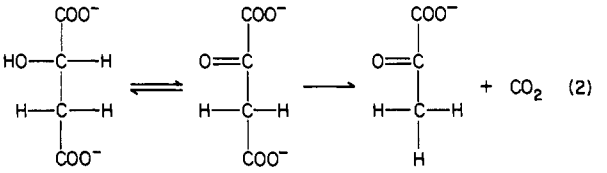

(2)

Hermes et al. (1982) used the multiple isotope effect method of examining the primary ^{13}C kinetic isotope effect with deuterated and unlabeled substrates to show that this mechanism was correct but were only able to establish limits on the intrinsic deuterium and ^{13}C isotope effects for the reaction.

Any intermediate generated in a chemical reaction will partition between reaction to give products and reversion to starting material according to the relative heights of the energy

† Supported by a grant from the National Institutes of Health (GM 18938).

[1] Abbreviations: TPN, triphosphopyridine nucleotide; TPNH, triphosphopyridine nucleotide, reduced; TPND, triphosphopyridine nucleotide, reduced, A-side deuterated; Acpyr-TPNH, 3-acetylpyridine adenine dinucleotide phosphate, reduced; Mes, 2-(*N*-morpholino)-ethanesulfonic acid; Pipes, 1,4-piperazinediethanesulfonic acid; Tricine, *N*-[tris(hydroxymethyl)methyl]glycine; mal, L-malate; pyr, pyruvate; EDTA, ethylenediaminetetraacetic acid.

0006-2960/85/0424-0944$01.50/0